High-order LES benchmarking of confined rotor-stator flows

Stéphane Viazzo, Anthony Randriamampianina, Sébastien Poncet, Patrick Bontoux, Eric Serre

High-order LES benchmarking of confined rotor-stator flows

S. Viazzo, A. Randriamampianina, S. Poncet, P. Bontoux and E. Serre.

Laboratoire M2P2, UMR 6181 CNRS / Aix-Marseille Université, Marseille, France.

Eric.Serre@L3m.univ-mrs.fr

Abstract

In many engineering and industrial applications the investigation of rotating turbulent flow is of great interest. In rotor-stator cavities, the centrifugal and the Coriolis forces have a strong influence on the turbulence by producing a secondary flow in the meridian plane composed of two thin boundary layers along the discs separated by a non-viscous geostrophic core. Some research has been done using RANS and URANS modelling, however, so far very few investigations have been done using LES. This paper reports on a benchmarking of two high-order LES modelling to predict a turbulent rotor-stator flow at rotational Reynolds number $Re(\Omega b^2/\nu)=4.10^5$. The dynamic Smagorinsky model for the subgrid-scale stress (Germano *et al*. 1991) is here compared to a spectral vanishing viscosity technique (Séverac and Serre 2006). Results show a good agreement in the predictions of the mean velocities and Reynolds stresses with experimental data with the largest discrepancy occurring in the prediction of the tangential normal stresses $R_{\theta\theta}$. These both LES modelling are among the firsts to catch the main features of the turbulent flow at this moderately high Reynolds number where rotor-layer goes to turbulence at a local radius close to the periphery. As already noticed by Wu and Squires (2000) on the single disk case, this work offers indirect supports to the idea that in such flows when large-scale motions are accurately resolved - the high-order schemes guarantying a weak dissipative truncation error - LES modelling seems to have only weak effects on the predictions.

1 Introduction

The simulation of turbulent rotating cavities flows is a major issue in computational fluid dynamics and engineering applications such as disk drives used for digital disk storage in computers, automotive disk brakes, and disks to support turbomachinery blades. Besides its primary concern to industrial applications (Owen and Rogers 1989), the rotor-stator problem has also proved a fruitful means of studying the effects of mean flow three-dimensionality on the turbulence and its structure (Little and Eaton 1994, Lygren and Anderson 2004, Kang et al., Séverac et al. 2007), since it is among the simplest flows where the boundary layers are three-dimensional from their inception.

RANS modelling of such flows has been deeply investigated in the group of B.E. Launder in Manchester for several decades (see a review in Launder *et al*. 2010). Conclusions of such investigations are that eddy viscosity models clearly fail by providing erroneous rotor-layer predictions and rotation rates in the central core, particularly due to a delay in the transition to turbulence along the rotor (Iacovides and Theofanoupolos, 1991). Second moment closures provide a more appropriate level of modelling (Launder and Tselepidakis, 1994; Poncet *et al.*, 2005b), but even if they provide a correct distribution of laminar and turbulent regions, the Reynolds stress behaviour is not fully satisfactory, particularly near the rotating disk.

Consequently, LES seems to be the appropriate level of modelling. Wu and Squires (2000) performed the first LES of the three-dimensional turbulent boundary-layer over a free rotating disk in an otherwise quiescent incompressible fluid at $Re = 6.5\times10^5$ and using periodic boundary conditions both in the radial and tangential directions. They concluded that when the grid is fine enough to resolve accurately large-scale motions, SGS models and further grid refinement have no significant effect on their LES predictions. Lygren and Andersson (2004) and Andersson and Lygren (2006) performed LES of the axisymmetric and statistically steady turbulent flow in an angular section of an unshrouded rotor-stator cavity for Reynolds numbers ranging from $Re = 4\times10^5$ to $Re = 1.6\times10^6$. Their study showed that the mixed dynamic subgrid scale model of Vreman *et al.* (1994) provided better overall results compared to the dynamic subgrid scale model of Lilly (1992). Finally, Séverac and Serre (2007) proposed a LES approach based on a spectral vanishing viscosity (SVV) technique, which showed to provide very satisfying results with respect to experimental measurements in an enclosed rotor-stator cavity including confinement effects and for Reynolds numbers up to one million (Séverac *et al.* 2007).

Clearly, traditional LES approaches using a fixed coefficient for subgrid scale viscous dissipation are not able to tackle the transition on the rotor-layer. In this work, it is replaced by the dynamic eddy-viscosity SGS model (SGS-LES) associated to a fourth-order

compact finite-difference scheme. (SGS-LES) results are then compared with spectral vanishing viscosity results formerly published in Séverac *et al.* (2007) in the same configuration. This alternative LES formulation (SVV-LES) associated to a spectral approximation is based on a modification of the Navier–Stokes equations which only dissipates the short length scales, a feature which is reminiscent of LES models, keeping the spectral convergence of the error (Séverac and Serre 2007).

The aim of this work is to evaluate LES modelling in a very complex configuration with both laminar and turbulent flow regions and involving confinement, flow curvature and rotation effects providing a strongly inhomogeneous and anisotropic turbulence within the boundary layers along the disks and the endwalls. The use of high-order numerical approximations guarantees here that the dissipative truncation error cannot act as an additional subgrid model.

First geometrical and numerical modellings are briefly described in Sections 2 and 3, respectively. Comparisons between the LES calculations and previous velocity measurements (Séverac *et al.* 2007) are performed for a given Reynolds number $Re=4\times10^5$ in Section 4 for the mean and turbulent fields. Finally some conclusions and closing remarks are provided in Section 5.

2 Geometrical modelling

The cavity (Figure 1) is composed by two parallel disks of radius b=140mm, one rotating at a uniform angular velocity Ω (rotor), one being at rest (stator). The disks are delimited by an inner cylinder (the hub) of radius a=40 mm attached to the rotor and by an outer stationary casing (the shroud) attached to the stator. The interdisk spacing, denoted h, is fixed here to 20 mm.

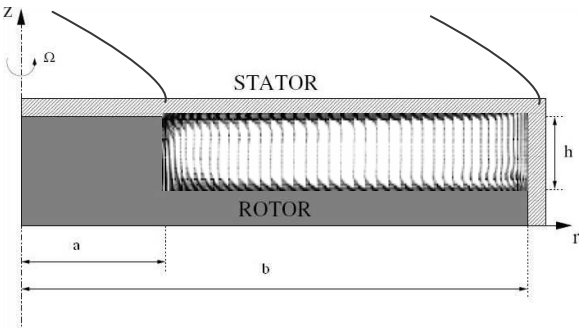

Figure 1: Rotor-stator cavity with relevant notations. Averaged velocity vector-field (LES-SVV) showing the secondary flow in the meridian plane at $Re=4.10^5$.

The mean flow is governed by three global control parameters: the aspect ratio of the cavity G, the curvature parameter R_m and the rotational Reynolds number Re based on the outer radius b of the rotating disk defined as follows:

$$G=\frac{b-a}{h}=5,\quad R_m=\frac{b+a}{b-a}=1.8,\quad \mathrm{Re}=\frac{\Omega b^2}{\nu}=4\times10^5 \quad (1)$$

where ν is the fluid kinematic viscosity. The values of the geometrical parameters were chosen in order to be relevant with industrial devices such as real stage of turbopump, and to satisfy technical constraints of the experimental device as well as computational effort to reach statistically converged states. In the experimental setup, a small clearance j=0.85 mm exists between the rotor and the shroud because of mechanical constraints. In the following, the stator is located at $z^*=z/h=1$ and the rotor at $z^*=0$. We define also the dimensionless radial location as $r^*=(r-a)/(b-a)$.

2 Numerical set up

The incompressible fluid motion is governed by the three-dimensional Navier-Stokes equations written in primitive variables for cylindrical coordinates (r,θ,z). No-slip boundary conditions are applied at all walls so that all the near-wall regions were explicitly computed. The tangential velocity is fixed to 0 on the stator and on the shroud and to the local disk velocity Ωr on the rotor and the hub. The singularities present in the experiments at the junctions between rotating and stationary walls are regularized in the two LES codes by using an exponential function to provide a smooth switchover.

Conservation equations are solved using a Fourier approximation in the homogeneous tangential direction. In both non homogeneous radial and vertical directions the solutions are approximated using either a fourth-order compact finite-difference scheme (Abide and Viazzo 2005) either a collocation-Chebyshev approximation (Séverac and Serre 2006).

In both numerical code, the time advancement is second-order accurate and is based on the explicit Adams–Bashforth time-stepping for the convective terms and an implicit Crank–Nicolson (LES-FD) or Euler-backward (LES-SVV) scheme for the viscous terms. The velocity-pressure coupling is solved using a two-step fractional scheme (predictor–corrector) reducing the problem at each time step to a set of two-dimensional Helmholtz equations (Raspo *et al.* 2002).

In the LES-FD, mass and momentum conservation is enforced for the large-scale resolved variables, which are obtained by grid-filtering the Navier-Stokes equations. The unresolved small scale turbulence is represented by a dynamic eddy-viscosity SGS model proposed by Lilly (1992) in which the Smagorinsky coefficient C_s is evaluated as a part of the solution at each time step using a test filter. As usually, the test filter width was twice the grid-filter width. The test filter used sequentially in each non

homogeneous direction is a symmetric discrete filter based on the trapezoidal rule as proposed in Sagaut (2005) while in the homogeneous direction a cutoff filter was applied with the Fourier approximation. Furthermore, negative values of ν_T are clipped to zero if the turbulent viscosity ν_T is negative meaning that no transfer of energy from the unresolved scales to the resolved ones (backscatter) is taken into account in order to be consistent with the LES-SVV model. Finally, in order to improve time-stability the eddy viscosity is split into an averaged value in the azimuthal direction treated semi-implicitly by the way of internal iterations and a fluctuation part treated fully explicitly. Practically, five iterations are required to obtain a convergence criterion of 10^{-6}.

In the LES-SVV, an appropriate viscosity kernel operator is incorporated in the conservation equations, only active for high wave numbers. This operator does not affect the large scales of the flow and stabilise the solution by increasing the dissipation, particularly near the cut off frequency without sacrificing the formal accuracy, i.e., exponential convergence, (Séverac and Serre 2007). A new diffusion operator Δ_{SVV} can be simply implemented by combining the classical diffusion and the new SVV terms to obtain:

$$\nu\Delta_{SVV} = \nu\Delta + \nabla.\left(\varepsilon_N Q_N \nabla\right) = \nu\nabla.S_N\nabla$$

where

$$S_N = diag\left\{S_N^i\right\}, S_N^i = 1 + \frac{\varepsilon_N^i}{\nu} Q_N^i$$

where $\varepsilon_{N_i}^i$ is the maximum of viscosity and Q_N^i is a 1D operator defined in the spectral space by an exponential function parameterized by ω_T^i the threshold after which, the viscosity is applied and ω_N^i is the highest frequency calculated in the direction i as:

$$\hat{Q}_N(\omega_n) = 0 \text{ for } 0 \le \omega_n \le \omega_T$$

$$\hat{Q}_N(\omega_n) = \varepsilon_N e^{-[(\omega_N-\omega_n)/(\omega_T-\omega_n)]^2} \text{ for } \omega_T \le \omega_n \le \omega_N$$

Because our SVV operator is fully linear, no additional computational cost is needed. The computational parameters used in the present LES-SVV are summed up in table 1, where δt is the time step.

direction	ω_T	ε_N	Grid
r	$0.8\ N^{1/2}$	1/(2N)	N=121
θ	$N^{1/2}$	1/(2N)	K=181
z	$N^{1/2}$	1/(2N)	M=65

Table 1: Parameters for the LES-SVV

In both simulations, the number of grid points is fixed 121×65×180 respectively in the radial, axial and azimuthal directions with a time step of $3.10^{-4}\Omega^{-1}$ for LES-FD and $5.10^{-5}\ \Omega^{-1}$ for (LES-SVV). The grid resolution was chosen from our former study using LES-SVV (Séverac *et al.* 2007) where results have shown a satisfactory agreement with the experimental measurements. Such a grid corresponds to an axial wall-coordinate z+ around unity slightly varying with r the total friction velocity increasing towards the periphery of the cavity.

Mean flow and second-order statistics were obtained through averaging over time as well as along the homogeneous tangential direction.

3 Results

Turbulent quantities have been compared to velocity measurements using a two component laser Doppler anemometer (LDA) from above the stator (see details in Séverac *et al.* 2007). About 5000 validated data are necessary to obtain the statistical convergence of the measurements. The mean and turbulent quantities are given with an accuracy of 2% and 5% respectively. Comparisons with the Reynolds Stress Modelling (RSM) of Elena and Schiestel (1995) are also provided. This model has been sensitized to the implicit effects of rotation on turbulence and applied to a wide range of flow conditions in enclosed or opened rotor-stator cavities (Poncet *et al.* 2005b).

The averaged velocity vector field is presented in Figure 1 and it is qualitatively similar to the laminar Batchelor flow obtained at much smaller rotation rates. Both LES-FD and LES-SVV provide the same base flow characterized by a strong circulation in the tangential direction and a secondary flow in the meridian plane due to centrifugal and Coriolis forces with two boundary layers developed on each disk separated by a central rotating core. There is no axial gradient in the core as a consequence of the Taylor-Proudman theorem. The fluid is pumped centrifugally outwards along the rotor and is deflected in the axial direction after impingement on the external cylinder. After a second impingement on the stator, it flows radially inwards along the stator, by conservation of mass, before turning along the hub and being centrifuged again by the rotating disk. The main effect of finite-radius disks and most of all of the inner and outer cylinders is that the boundary conditions are not compatible with self-similarity solutions though there may be qualitative resemblance far from the end walls. Thus, the thicknesses of the Ekman layer on the rotor and of the Bödewadt layer on the stator are not constant along the radius within the cavity. Note that the Bödewadt layer is almost twice thicker than the Ekman layer.

Quantitative comparisons have been made at mid-radius of the cavity that corresponds to a local Reynolds number $Re_r=1.65\times10^5$, for which the stator boundary layer is turbulent, whereas the rotor one is only weakly turbulent according to the experiments of Itoh *et al.* (1992). Figure 2 shows the axial profiles of the mean radial $V_r^*=V_r/(\Omega r)$ and tangential $V_\theta^*=V_\theta$

/ (Ωr) velocity components at mid-radius r^*=0.5 normalized by the rotor velocity. The axial profile of the mean axial velocity component is not shown here because it is around zero far from the inner and outer cylinders. A crucial quantity for engineering applications is the entrainment coefficient of the fluid or the core swirl ratio K= $(V_\theta/(\Omega r))_{core}$ because it is directly linked to the radial pressure gradient in the cavity and as a consequence to the axial thrusts applied on the rotor (Poncet *et al.* 2005a). The LES-FD clearly underestimates K predicting K=0.32 at r^*=0.5 with respect to K=0.36 given by LES-SVV as well as experimental measurements. This underestimate value is of the same order that the value K=0.315 predicted by the RSM and very close to the value obtained with the laminar similarity solution, K=0.313, by Pearson (1965) for infinite-disk cavities.

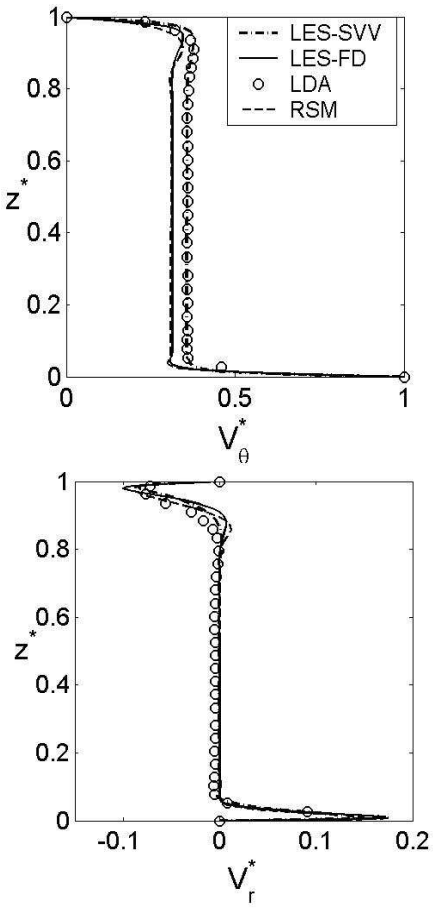

Figure 2: Mean profiles of tangential and radial component of velocity normalized by the local speed of the disk at mid-radius. Comparisons between the LES-SVV (-·-), the LES-FD (—), the LDA measurements (o) and the RSM model (- -).

Both LES-SVV and LES-FD predict quite well the thickness of the Ekman layer on the rotor at mid-radius which is characteristic of a weakly turbulent layer at this radial location. The LES-SVV slightly underestimates the thickness of the Bödewadt layer but provides better overall results than the LES-FD and the RSM. The V_r*-profile deduced from the RSM model as well as the LES-FD exhibits a local extremum around z^*=0.8 characteristic of laminar boundary layers.

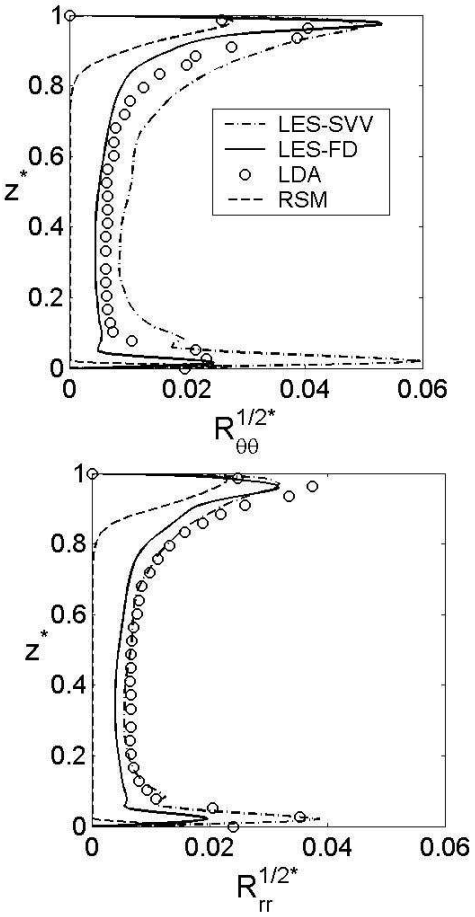

Figure 3**:** Axial profiles of the two main Reynolds stress tensor components at mid-radius. Comparisons between the LES-SVV (-·-), the LES-FD (—), the LDA measurements (o) and the RSM model (- -).

Second-order statistics available from experimental measurements in the radial $R_{rr} = \overline{v_r'^2}/(\Omega r)^2$ and tangential directions $R_{\theta\theta} = \overline{v_\theta'^2}/(\Omega r)^2$ have been computed in Figure 3. The other three shear-stresses are of negligible importance, with a magnitude two-order lower than the previous Reynolds stresses, as already obtained in DNS by Lygren and Andersson (2000). LES results provide an overall agreement with the experimental data as well in the boundary layers as in the core. LES-FD underpredicts the turbulence intensity more largely than the LES-SVV. As expected, RSM underpredicts the turbulence intensity in both directions as well in the core as in both boundary layers. The peaks of the normal stresses maxima are relatively well predicted within the stator layer for both radial and tangential directions; at a distance from the stator equal to 0.05h for the radial component and two times closer 0.025h for the tangential component. Both LES-SVV and LES-FD tend to overpredict $R_{\theta\theta}$ in both boundary layers,

the maximum being reached by the LES-SVV within the rotor layer. As a consequence, the anisotropy of the normal stresses is stronger in LES than in experiment. Such behaviour could be related to the anisotropy of the grid computation, which is globally much coarser in the tangential, especially at large radii. This idea would be supported by the LES of Wu and Squires (2000) which observed a strong sensitivity of this component depending on the resolution.

Qualitatively both LES-FD and LES-SVV predict the same structures within both boundary layers. On Figure 4, the structures are localized within the boundary layers as shown by the isocontours of the Q-criterion. It is interesting to notice the network of spiral arms along the inner cylinder which change of inclination at about mid-height under the influence of the centrifugal or centripetal boundary layers along the disks.

Figure 4: Iso-surfaces of the Q-criterion and iso-lines in the meridian planes. LES-FD.

Figures 5 and 6 present iso-surfaces of the Q-criterium along both disks. As observed on the turbulence statistics the rotating disk layer is only weakly turbulent featured by coherent positive spiral arms (as they roll up in the rotation sense of the disk) at intermediate radii (Figures 5a and b). These structures are characteristic of the Type I instability (cross-flow instability), which plays an important role in the transition process to turbulence. Around the hub where the flow coming from the stator impinges the rotor, both simulations predict a highly turbulent region with smaller disorganized structures.

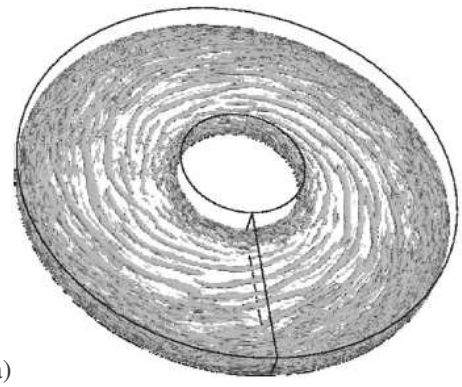

(a)

(b)

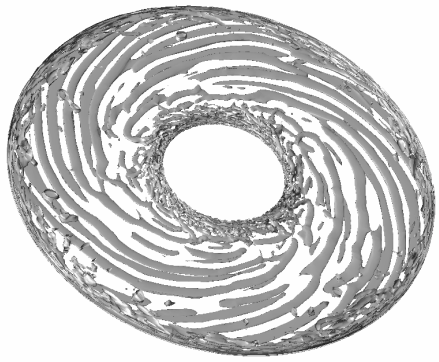

Figure 5**:** Iso-surfaces of the Q-criterion along the rotor: (a) LES-SVV (b) LES-FD. The rotating disk rotates counter-clockwise.

Moreover, only the LES-SVV is able to predict the transition to turbulence expected by theory and experiments at large radii corresponding at a local Reynolds $Re_r^{1/2}$ = 386: the spiral arms breakdown into smaller more concentric structures.

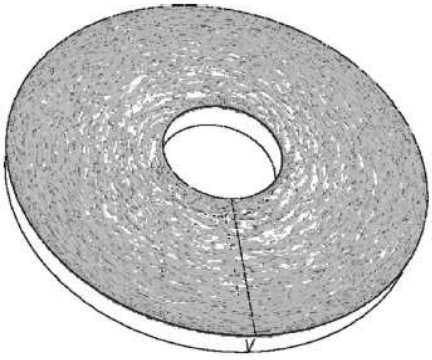

(a)

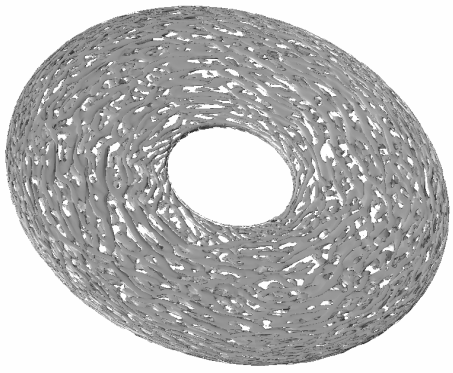

(b)

Figure 6**:** Iso-surfaces of the Q-criterion along the stator: (a) LES-SVV (b) LES-FD. The rotating disk rotates counter-clockwise.

Along the stationary disk, both LES exhibit very thin coherent vortical structures aligned with the

tangential direction (Figure 6) which is typical of a turbulent boundary layer. The thinner structures predict by the LES-SVV indicate nevertheless a globally higher level of turbulence.

5- Concluding remarks

These both LES modelling are among the firsts to catch the main features of the turbulent flow at this moderately high Reynolds number where stator layer is fully turbulent while rotor-layer goes to turbulence at a local radius close to the periphery. Results show a global good agreement in the predictions of turbulence quantities as well as flow structures. Nevertheless, the LES-SVV seems to provide better overall results compared to the LES-FD by providing a better global level of turbulence intensity with respect to LDA measurements and by predicting, at a location in good agreement with theory, transition to turbulence on the rotor. This work offers indirect supports to the idea that when using high-order numerical method (low numerical dissipation) the influence of the LES modelling in complex flows seems weaker. Such behaviour should encourage the LES community to increase its effort not only on the SGS modelling but also in the use of high-order schemes.

Acknowledgements

LES-SVV was granted access to the HPC resources of IDRIS under the allocation 2009-0242 made by GENCI (Grand Equipement National de Calcul Intensif). The LES-FD calculations have been performed on the M2P2 cluster composed of 2 Xeon quadcore 3 GHz. The work was supported by CNRS in the frame of the DFG-CNRS program “LES of complex flows”.

References

Abide S. and Viazzo S. (2005), A 2D compact fourth-order projection decomposition method, *J. Comp. Phys.*, Vol. 206, pp. 252-276.

Andersson H.I. and Lygren M. (2006), LES of open rotor-stator flow, *Int. J. Heat Fluid Flow* Vol.27, pp.551-557.

Elena L. and Schiestel R. (1995), Turbulence modeling of confined flow in rotating disk systems, *AIAA J.* Vol. 33 (5), pp.812-821.

Germano M., Piomelli U., Moin P. and Cabot W.H. (1991), A dynamic subgrid-scale eddy viscosity model, *Phys. Fluids A* Vol.3(7), pp.1760-1765.

Iacovides H. and Theofanoupolos I.P. (1991), Turbulence modelling of axisymmetric flow inside rotating cavities, *Int. J. Heat Fluid Flow* Vol. 12, p.2-11.

Itoh M., Yamada Y., Imao S. and Gonda M. (1992), Experiments on turbulent flow due to an enclosed rotating disc, *Exp. Thermal Fluid Sci.* Vol. 5, pp.359-368.

Launder B.E. and Tselepidakis, D.P. (1994), Application of a new second moment closure to turbulent channel flow rotating in orthogonal mode, *Int. J. Heat Fluid Flow* Vol. 15, pp.2-10.

Lilly D.K. (1992), A proposed modification of the Germano subgrid-scale closure method. *Phys. Fluids A* Vol. 4, pp.633–635.

Lygren M. and Andersson H. (2004), Large eddy simulation of the turbulent flow between a rotating and a stationary disk, *ZAMM* Vol. 55, pp.268-281.

Owen J. M. and Rogers R.H. (1989), Flow and heat transfer in rotating-disc systems, Vol. 1: Rotor-stator sytems, *Research Studies Press*, Taunton.

Pearson CE. (1965), Numerical solutions for the time-dependent viscous flow between two rotating coaxial disks. *J. Fluid Mech.* Vol. **21 (4)**, pp.623-33.

Poncet S., Chauve M.-P. and Le Gal P. (2005a), Turbulent Rotating Disk Flow with Inward Throughflow, *J. Fluid Mech.*, Vol. 522, p.253-262.

Poncet S., Chauve M.-P. and Schiestel R. (2005b), Batchelor versus Stewartson flow structures in a rotor-stator cavity with throughflow, *Phys. Fluids* Vol. 17, 075110.

Raspo I., Hugues S., Serre E., Randriamampianina A. and Bontoux P. (2002), Spectral projection methods for the simulation of complex three-dimensional rotating flows, *Comp. Fluids* Vol. 31, pp.745-767.

Sagaut P. (2005), Large Eddy Simulation for incompressible flows, 3rd Edition, Springer.

Schiestel R. and Viazzo S. (1995), A Hermitian–Fourier numerical method for solving the incompressible Navier–Stokes equations. *Comp. Fluids* Vol. 24, pp. 739–752.

Séverac E. and Serre E. (2007), A spectral vanishing viscosity for the LES of turbulent flows within rotating cavities, *J. Comp. Phys.* Vol. 226 (2), pp.1234-1255.

Séverac E., Poncet S., Serre E. and Chauve M.-P. (2007), Large eddy simulation and measurements of turbulent enclosed rotor-stator flows, *Phys. Fluids* Vol. 19, 085113.

Vreman B., Geurts B. and Kuerten H. (1994), On the formulation of the dynamic mixed subgrid-scale model. *Phys. Fluids* Vol. 6, pp.4057–4059.

Wu X. and Squires K.D. (2000), Prediction and investigation of the turbulent flow over a rotating disk, *J. Fluid. Mech.* Vol. 418, pp.231-264.